Aalborg Universitet

AALBORG UNIVERSITY
DENMARK

Virtual Drive Testing Over-The-Air for Vehicular Communications

Ji, Yilin; Fan, Wei; Nilsson, Mikael; Hentilä, Lassi; Karlsson, Kristian; Tufvesson, Fredrik; Pedersen, Gert Frølund

Publication date:
2020

Document Version
Accepted author manuscript, peer reviewed version

Link to publication from Aalborg University

Virtual Drive Testing Over-The-Air for Vehicular Communications

Yilin Ji, Wei Fan, Mikael Nilsson, Lassi Hentilä, Kristian Karlsson, Fredrik Tufvesson, and Gert Frølund Pedersen

Abstract—Multiple-input multiple-output (MIMO) over-the-air (OTA) testing is a standardized procedure to evaluate the performance of MIMO-capable devices such as mobile phones and laptops. With the growth of the vehicle-to-everything (V2X) service, the need for vehicular communication testing is expected to increase significantly. The so-called multi-probe anechoic chamber (MPAC) setup is standardized for MIMO OTA testing. Typically, a test zone of 0.85 wavelength in diameter can be achieved with an 8-probe MPAC setup, which can encompass device-under-test (DUT) of small form factors. However, a test zone of this size may not be large enough to encompass DUTs such as cars. In this paper, the sufficient number of OTA probes for the MPAC setup for car testing is investigated with respect to the emulation accuracy. Our investigation shows that the effective antenna distance of the DUT is more critical than its physical dimensions to determine the required number of OTA probes. In addition, throughput measurements are performed under the standard SCME UMa and UMi channel models with the 8-probe MPAC setup and the wireless cable setup, i.e. another standardized testing setup. The results show reasonably good agreement between the two setups for MIMO OTA testing with cars under the standard channel models.

Index Terms—V2X, LTE-V, channel modeling, MIMO OTA testing, MPAC, and wireless cable.

I. INTRODUCTION

A. Background of MIMO OTA Testing

Virtual drive testing (VDT) refers to evaluating the radio performance of wireless devices in laboratory environments [1]. Compared to unpredictable and expensive field trials in open environment, it allows for testing in more controllable and reproducible conditions. Within the context of VDT, multiple-input multiple-output (MIMO) over-the-air (OTA) testing is a standardized procedure to perform testing for MIMO-capable devices. It helps the manufacturers identify potential design flaws and production defects during the early-stage prototyping, mid-term refinement, and final massive roll-out.

Basically, three main types of MIMO OTA testing setups are defined in the standard [1], namely the multi-probe anechoic chamber (MPAC) setup, the wireless cable setup, and the reverberation chamber (RC) setup. The purpose of MIMO OTA

Yilin Ji, Wei Fan, and Gert Frølund Pedersen are with Antenna Propagation and Millimeter-wave Systems (APMS) section at Department of Electronic Systems, Aalborg University, Denmark. (Corresponding author: Wei Fan. Email: wfa@es.aau.dk)

Mikael Nilsson is with Volvo Car Corporation, Gothenburg, Sweden.

Lassi Hentilä is with Keysight Technologies Oy, Finland.

Kristian Karlsson is with Technical Research Institute of Sweden, Sweden.

Fredrik Tufvesson is with Department of Electrical and Information Technology, Lund University, Sweden.

testing is to evaluate the radio performance of device-under-test (DUT) under target propagation channels. Therefore, the key difference between different testing setups, besides the cost in complexity and expense, can be viewed in terms of the capability of emulating target channels.

The MPAC setup utilizes a channel emulator and a set of OTA probes to emulate target channels. The challenge of the MPAC setup usually occurs for emulating the target power angle spectrum (PAS) on the DUT side with OTA probes. The so-called test zone of an MPAC setup is defined as a geometric area where the target spatial correlation, i.e. the Fourier transform of the PAS, on the DUT side can be well approximated. The size of the test zone is determined mainly by the number of OTA probes with its diameter approximately proportional to the number of OTA probes [2]. Another terminology, namely the quiet zone, is also important to the MPAC setup, and it is often used in antenna measurement. It is defined as the geometric area where the field is homogeneous, and it is determined by the measurement range and reflectivity level. Note that in this study we focus on the test zone where channel spatial profiles can be controlled.

The wireless cable setup [3], also called the radiated two-stage (RTS) setup, utilizes a channel emulator to emulate target channels. The principle of the wireless cable setup is similar to that of the conducted two-stage setup except that the cable connections between the channel emulator output ports and the DUT antenna ports are realized over the air, and hence the name wireless cable. The quality of the realized wireless cable connections is measured by the isolation level. An ill-conditioned transfer function between the channel emulator output ports and the DUT antenna ports, e.g. in the case where the DUT antennas are closely located, may limit the achievable isolation level. In addition, the DUT antenna pattern is implemented numerically in the channel emulator, so the wireless cable setup is not capable of testing DUT with active antenna arrays. Therefore, the wireless cable setup is not a true end-to-end testing method as the MPAC setup.

Finally, the RC setup utilizes a metallic cavity and stirrers to generate isotropic spatial channels with Rayleigh fading due to the rich multipaths in the RC [4], [5]. Therefore, it is not as capable of generating arbitrary channel models as the MPAC and the wireless cable setup.

B. Problem Statement

Long term evolution for vehicles (LTE-V) has been proposed to embody the vehicle-to-everything (V2X) service defined in the standardization group 3GPP [6]. With the LTE-V technology, it is expected to make road traffic safer and

more efficient. A key component to enable the V2X service is a high-quality communication for vehicles. To assess the communication performance of the LTE-V during design phase, LTE mobile phones connected with external test antennas, e.g. shark-fin antennas, can be used to perform the standard MIMO OTA testing.

Since shark-fin antennas are usually mounted on car roofs for a clear field of view, potentially the roof also participates in the antenna radiation, which leads to induced surface currents being distributed on it. In such cases, the effective antenna distance of the DUT can be larger than the physical distance between the DUT antennas. However, depending on the specific radiation pattern of the DUT antennas, it is also possible that the induced surface currents concentrate only in the vicinity of the DUT antennas. Consequently, the resulting effective antenna distance can be much smaller than the dimension of the whole car, i.e. the upper bound of the effective antenna distance.

For the MPAC setup, it is required that the underlying test zone is larger than the effective antenna distance. There is a strong need in the industry to find out to which extent the presence of cars will affect the effective antenna distance, or equivalently the required size of the test zone, since a smaller test zone leads to a smaller number of required OTA probes and hence a lower system cost of the MPAC setup. To the best of our knowledge, this is still remained unknown in the literature.

C. State-of-the-art

The state-of-the-art on OTA testing for vehicles can be found for testing methodology verification [7]–[12] and vehicular channel models [12]–[15], respectively. In [7], an experiment with a car under a multi-probe setup in an open area was performed, and it was found the coupling from the OTA probes and the reflection and diffraction from cars are negligible, which verified the effectiveness of the quiet zone of the multi-probe setup for car testing. In [8], antenna correlation on cars was investigated with 3 OTA probes, and the measurements showed the similarity with the theoretical antenna correlation to some extent. In [9], an isolation level of about $40\,\mathrm{dB}$ was achieved experimentally for a wireless cable setup with 6 OTA probes in a radio-frequency (RF) shielded room, which demonstrated the achievable quality of wireless cable connections for cars. In [10], throughput measurements for cars were performed in a semi-anechoic chamber, where the ground was not covered by absorber, with a single OTA probe under single-path line-of-sight (LoS) channels. In [11], a plane-wave generator (PWG) solution was reported as an alternative for the compact antenna test range (CATR) setup [12] under single-path LoS channels. In [13], discussion was given on the properties of vehicular channels, and measurement-based path loss and shadowing models were proposed for vehicle-to-vehicle (V2V) communication in highway and urban scenarios in [14], [15]. However, to the best of our knowledge, investigation on MIMO OTA testing for cars with the MPAC and the wireless cable setup under the standardized channel models is still missing in the literature.

D. Contribution

In this paper, the principles of the MPAC and the wireless cable method for MIMO OTA testing are briefly revisited. Three DUT setups are used for testing with supposedly different effective antenna distances. For the MPAC method, the sufficient number of OTA probes for different DUT setups is synthetically investigated in terms of the emulation accuracy based on three metrics, i.e. the average received power, branch power ratio, and antenna correlation at the DUT side. For the wireless cable method, the isolation level between connections is used to evaluate the emulation accuracy, and the achieved values in the measurements are shown. Finally, throughput measurements are performed with the two methods under standard channel models, and comparison between the results is made.

The main contribution of the paper lies in the following aspects:

- The sufficient size of the test zone, or equivalently the sufficient number of OTA probes, is synthetically investigated for cars with the MPAC setup.
- Throughput measurements are performed for cars with the MPAC and the wireless cable setup, and comparison between the results is presented.

The rest of the paper is structured as follows: Section II introduces the principle of the MPAC and the wireless cable method for MIMO OTA testing. The metrics to evaluate the emulation accuracy for the MPAC and the wireless cable setup are also given in Section II. Section III describes the measurement campaign with the detailed setup and setting information. Section IV presents the obtained values for the emulation accuracy metrics and the measured throughput results. Section V concludes the paper.

II. PRINCIPLE OF OTA METHODS

A. The Target Channel Model

In the current standard [1], the channel model mostly used for MIMO OTA testing is the Spatial Channel Model Extended (SCME) including Urban Macro-cell (UMa) and Urban Micro-cell (Umi) scenarios [16]. The SCME model belongs to the family of geometry-based stochastic channel models (GSCM) [17]–[19]. Within the context of GSCMs, propagation channels are modelled as the superposition of a number of propagation paths, and paths having similar propagation parameters are further grouped into clusters to lower the model complexity.

Given a MIMO communication system with S transmit (Tx) antennas and U receive (Rx) antennas, the time-variant channel transfer function from the sth Tx antenna to the uth Rx antenna can be expressed as [19]

$$h_{u,s}(t,f) = \sum_{n=1}^{N} h_{u,s,n}(t,f), \qquad (1)$$

where t and f denote the time and the frequency, respectively. The subscript n is the index of the cluster and N the total
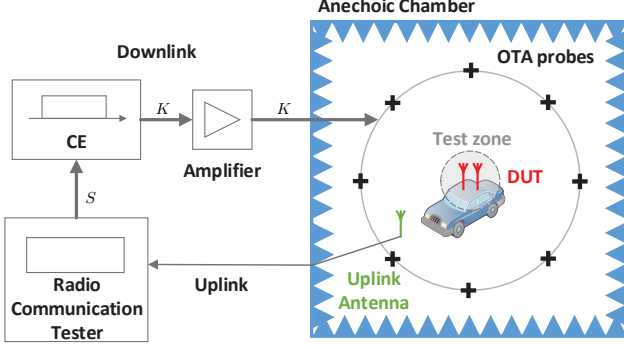
Fig. 1. The diagram of MIMO OTA testing with an MPAC setup. S is the number of Tx antennas, and K is the number of dual-polarized OTA probes. Acronyms: channel emulator (CE).

number of clusters. The contribution of the nth cluster can be further expressed as

$$h_{u,s,n}(t,f) = \sqrt{\frac{P_n}{M}} \sum_{m=1}^{M} \begin{bmatrix} F_{s,\mathrm{Tx}}^{\mathrm{V}}(\phi_{n,m}) \\ F_{s,\mathrm{Tx}}^{\mathrm{H}}(\phi_{n,m}) \end{bmatrix}^{\mathrm{T}} \boldsymbol{A} \begin{bmatrix} F_{u,\mathrm{Rx}}^{\mathrm{V}}(\theta_{n,m}) \\ F_{u,\mathrm{Rx}}^{\mathrm{H}}(\theta_{n,m}) \end{bmatrix}$$
$$\cdot \exp(j2\pi \upsilon_{n,m}t) \cdot \exp(-j2\pi f\tau_n), \qquad (2)$$

where m is the index of the path of a cluster, and $\upsilon_{n,m}$, $\theta_{n,m}$, and $\phi_{n,m}$ denote the Doppler frequency, the angle of arrival (AoA), and the angle of departure (AoD) of the (n,m)th path, i.e. the mth path of the nth cluster, respectively. M is the total number of paths in a cluster. P_n and τ_n are the power and the delay of the nth cluster, respectively. The terms $F_{u,\mathrm{Rx}}^{\mathrm{V}}(\cdot)$ and $F_{u,\mathrm{Rx}}^{\mathrm{H}}(\cdot)$ are the complex radiation pattern of the uth Rx antenna in the vertical (V) and the horizontal (H) polarization, respectively. Similarly, $F_{s,\mathrm{Tx}}^{\mathrm{V}}(\cdot)$ and $F_{s,\mathrm{Tx}}^{\mathrm{H}}(\cdot)$ are those of the sth Tx antenna in the V and the H polarization, respectively. Furthermore, $\boldsymbol{A}$ is the polarization matrix which reads

$$\boldsymbol{A} = \begin{bmatrix} \exp\left(j\Phi_{n,m}^{\mathrm{VV}}\right) & \sqrt{\kappa_{n,m}^{-1}} \exp\left(j\Phi_{n,m}^{\mathrm{VH}}\right) \\ \sqrt{\kappa_{n,m}^{-1}} \exp\left(j\Phi_{n,m}^{\mathrm{HV}}\right) & \exp\left(j\Phi_{n,m}^{\mathrm{HH}}\right) \end{bmatrix}, \qquad (3)$$

where $\Phi_{n,m}^{\mathrm{VV}}$, $\Phi_{n,m}^{\mathrm{VH}}$, $\Phi_{n,m}^{\mathrm{HV}}$, and $\Phi_{n,m}^{\mathrm{HH}}$ are the initial phases of the (n,m)th path for the vertical-to-vertical (VV), the horizontal-to-vertical (HV), the vertical-to-horizontal (VH), and the horizontal-to-horizontal (HH) polarizations, respectively. Moreover, they are usually characterized as independent and identical distributed (i.i.d.) random variables following the uniform distribution over $[0, 2\pi]$. $\kappa_{n,m}$ is the cross-polarization ratio (XPR) of the (n,m)th path.

B. The MPAC Based Methods

1) Principle: The MPAC based methods generally include two specific methods called the prefaded signals synthesis (PFS) and the plane wave synthesis (PWS), respectively. The detailed emulation principle can be found in [2]. Here we briefly describe that of the PFS method, which is more commonly used in practice in the industry.

The PFS method is developed based on the wide-sense stationary uncorrelated scattering (WSSUS) assumption [20]

for the target channel model. Since the parameters of the target channel are time-invariant and the initial phases of the (n,m)th path are i.i.d. random variables, the target channel model fulfils the WSSUS assumption, with which the channel can be fully characterized by its second-order statistics, i.e. the correlation functions in the respective domains of the channel [21].

A typical MPAC setup is shown in Fig. 1. For the downlink, test signals are sent from a radio communication tester, e.g. a base station emulator, through coaxial cables to a channel emulator. The test signals are convolved with the channel in the channel emulator so the prefaded signals are generated. Further, the signals are amplified and fed to the OTA probes. Finally, the emulated channel complied with the target channel is generated in the test zone to test the DUT. For the uplink, the uplink antenna picks up the signal from the DUT and sends it back to the radio communication tester.

For an MPAC setup with K dual-polarized OTA probes, the fading sequences corresponding to the nth cluster fed to the kth OTA probe antenna can be expressed as [2], [22]

$$h_{k,s,n}^{\mathrm{V}}(t,f) = \sqrt{\frac{P_n}{M}} \sum_{m=1}^{M} \begin{bmatrix} F_{s,\mathrm{Tx}}^{\mathrm{V}}(\phi_{n,m}) \\ F_{s,\mathrm{Tx}}^{\mathrm{H}}(\phi_{n,m}) \end{bmatrix}^{\mathrm{T}} \boldsymbol{A}_k \begin{bmatrix} 1 \\ 0 \end{bmatrix} \cdot \sqrt{g_{k,n}}$$
$$\cdot \exp(j2\pi \upsilon_{n,m}t) \cdot \exp(-j2\pi f\tau_n), \qquad (4)$$

$$h_{k,s,n}^{\mathrm{H}}(t,f) = \sqrt{\frac{P_n}{M}} \sum_{m=1}^{M} \begin{bmatrix} F_{s,\mathrm{Tx}}^{\mathrm{V}}(\phi_{n,m}) \\ F_{s,\mathrm{Tx}}^{\mathrm{H}}(\phi_{n,m}) \end{bmatrix}^{\mathrm{T}} \boldsymbol{A}_k \begin{bmatrix} 0 \\ 1 \end{bmatrix} \cdot \sqrt{g_{k,n}}$$
$$\cdot \exp(j2\pi \upsilon_{n,m}t) \cdot \exp(-j2\pi f\tau_n), \qquad (5)$$

for the V and the H polarization, respectively. In (4) and (5), $g_{k,n}$ with $\sum_{k=1}^{K} g_{k,n} = 1$ is the power weight applied at the kth OTA probe for the nth cluster. Moreover, $\boldsymbol{A}_k$ is the polarization matrix for the kth OTA probe, which reads

$$\boldsymbol{A}_k = \begin{bmatrix} \exp\left(j\Phi_{n,m,k}^{\mathrm{VV}}\right) & \sqrt{\kappa_{n,m}^{-1}} \exp\left(j\Phi_{n,m,k}^{\mathrm{VH}}\right) \\ \sqrt{\kappa_{n,m}^{-1}} \exp\left(j\Phi_{n,m,k}^{\mathrm{HV}}\right) & \exp\left(j\Phi_{n,m,k}^{\mathrm{HH}}\right) \end{bmatrix}, \qquad (6)$$

where $\Phi_{n,m,k}^{\mathrm{VV}}$, $\Phi_{n,m,k}^{\mathrm{VH}}$, $\Phi_{n,m,k}^{\mathrm{HV}}$, and $\Phi_{n,m,k}^{\mathrm{HH}}$, similar to those in (3), are also i.i.d. random variables following the uniform distribution over $[0, 2\pi]$, respectively. We can see in (4) and (5) that the parameter domains of the target channel, i.e. the delay, Doppler frequency, AoD, and polarizations, are implemented in the channel emulator and with the dual-polarized OTA probes. Therefore, the core of the PFS method is to emulate the target PAS on the DUT side, or alternatively its Fourier transform dual, the spatial correlation on the DUT side by applying a proper set of $g_{k,n}$. The set of $g_{k,n}$ can be solved by minimizing the difference between the spatial correlation of the emulated channel and that of the target channel through convex optimization in the test zone [2]. The emulated channel

for the nth cluster from the sth Tx antenna to the uth DUT antenna can be written as

$$\hat{h}_{u,s,n}(t,f)$$
$$= \sum_{k=1}^{K} \left\{ F_{u,\mathrm{Rx}}^{\mathrm{V}}(\theta_k) \cdot h_{k,s,n}^{\mathrm{V}}(t,f) + F_{u,\mathrm{Rx}}^{\mathrm{H}}(\theta_k) \cdot h_{k,s,n}^{\mathrm{H}}(t,f) \right\}, \tag{7}$$

which shares the common second-order statistics with the target channel $h_{u,s,n}(t,f)$ [21].

2) Metrics of Emulation Accuracy for the MPAC Method: Given the DUT antenna radiation pattern, we can calculate metrics such as the average received power, the branch power ratio, and the antenna correlation at the DUT side under the target and the emulated channel, respectively, to evaluate the emulation accuracy [22].

Taking a 2×2 MIMO system for example, the average received power at the uth Rx branch with $u = \{1, 2\}$, under the target channel can be calculated as

$$\bar{P}_u = \mathbb{E}_t \left\{ \sum_s \left| \sum_\tau H_{u,s}(t,\tau) \right|^2 \right\}, \tag{8}$$

where $\mathbb{E}_t\{\cdot\}$ is the averaging operator over time t, $|\cdot|$ is the modulus operator, and $H_{u,s}(t,\tau)$ is the time-variant channel impulse response in the delay τ domain transformed from $h_{u,s}(t,f)$ through inverse Fourier transform.

The branch power ratio between the two Rx antennas can be further calculated as

$$\Delta \bar{P} = \left| 10 \log_{10}(\bar{P}_1) - 10 \log_{10}(\bar{P}_2) \right|. \tag{9}$$

Similarly, by replacing the target channel with the emulated channel in (8), we can obtain the average received power and the branch power ratio for the emulated channel.

The complex-valued antenna correlation between the two Rx antennas with respect to the sth Tx antenna with $s = \{1, 2\}$ can be calculated as [8]

$$\rho_s = corr\left(\sum_\tau H_{1,s}(t,\tau), \sum_\tau H_{2,s}(t,\tau) \right)$$
$$= \frac{\mathbb{E}_t\left\{ \sum_\tau H_{1,s}(t,\tau) \cdot \sum_{\tau'} H_{2,s}(t,\tau')^* \right\}}{\sqrt{\mathbb{E}_t\left\{ |\sum_\tau H_{1,s}(t,\tau)|^2 \right\} \cdot \mathbb{E}_t\left\{ |\sum_{\tau'} H_{2,s}(t,\tau')|^2 \right\}}}, \tag{10}$$

where $corr(\cdot, \cdot)$ denotes the Pearson correlation, and $(\cdot)^*$ is the complex conjugate. Since the antenna gain pattern is the same between the two assumed base station (BS) antennas [1], the antenna correlation between the Rx antennas is irrelevant to the Tx antennas, i.e. $\rho_1 = \rho_2$.

C. The Wireless Cable Method

1) Principle: The wireless cable method is another way to replace the traditional conducted testing method. The block diagrams of the conducted testing method and the wireless cable method are shown in Fig. 2. For the conducted testing, the test signals $\boldsymbol{x}(t,f) \in \mathbb{C}^{S \times 1}$ are sent from a base station emulator to the channel emulator via RF coaxial cables. After convolving with the target channel $\boldsymbol{H}(t,f) = \{h_{u,s}(t,f)\} \in$
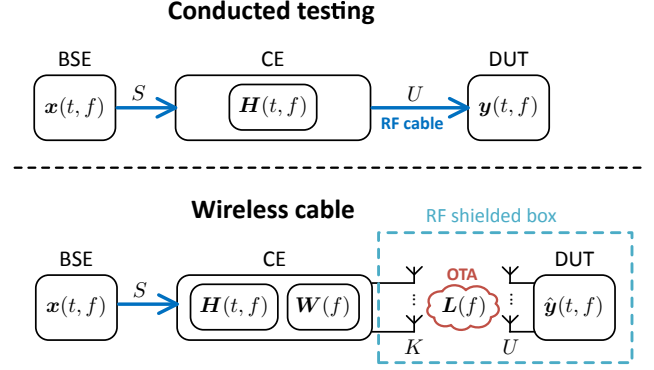

Fig. 2. The block diagrams of the conducted testing method and the wireless cable method. S and U are the number of Tx and Rx antennas, respectively. K is the number of OTA probes. Acronyms: base station emulator (BSE), channel emulator (CE).

$\mathbb{C}^{U \times S}$ as in (1), the faded signals $\boldsymbol{y}(t,f) \in \mathbb{C}^{U \times 1}$ are forwarded to the DUT, again via cables. The signal model for the conducted method can be written as

$$\boldsymbol{y}(t,f) = \boldsymbol{H}(t,f) \cdot \boldsymbol{x}(t,f). \tag{11}$$

For the wireless cable method, a weighting matrix $\boldsymbol{W}(f) \in \mathbb{C}^{K \times S}$ is generated in the channel emulator in addition to the target channel $\boldsymbol{H}$. The signals output from the channel emulator are first radiated via K OTA probes. The signals then propagate over the air with a transfer function $\boldsymbol{L}(f) \in \mathbb{C}^{U \times K}$. Lastly they are received by the U DUT antennas. An RF shielded box is used to exclude interference from the environment. The signal model for the wireless cable method can be written as

$$\hat{\boldsymbol{y}}(t,f) = \boldsymbol{L}(f) \cdot \boldsymbol{W}(f) \cdot \boldsymbol{H}(t,f) \cdot \boldsymbol{x}(t,f). \tag{12}$$

The weighting matrix $\boldsymbol{W}$ is designed so that $\boldsymbol{L}(f) \cdot \boldsymbol{W}(f)$ approximates an identity matrix $\boldsymbol{I}_U \in \mathbb{C}^{U \times U}$, and hence $\hat{\boldsymbol{y}}$ approximates $\boldsymbol{y}$. Note that $\boldsymbol{L}(f)$ and $\boldsymbol{W}(f)$ are usually evaluated at center frequencies for narrowband systems. If the transfer function $\boldsymbol{L}$ is known, $\boldsymbol{W}$ can be easily solved by the least squares method. Note that $K \geq U$ is required, and it is a necessary but insufficient condition to obtain a unique solution of $\boldsymbol{W}$ [3]. However, knowing $\boldsymbol{L}$ requires that the DUT is able to report the transfer function, which is not a common feature of current user terminals. Therefore, the transfer function $\boldsymbol{L}$ is typically unavailable in practice. In this case, methods for determining $\boldsymbol{W}$ with the average received power level, e.g. the reference signal received power (RSRP) in LTE, have been developed [3].

2) Metrics of Emulation Accuracy for the Wireless Cable Method: Consider a 2×2 MIMO system with $K = 4$ OTA probes for example to establish the wireless cable connections. Due to the maximum rank of the weighting matrix $\boldsymbol{W} \in \mathbb{C}^{4 \times 2}$ is 2, one way to formulate $\boldsymbol{W}$ can be found in [3] as

$$\boldsymbol{W} = \begin{bmatrix} 1 & 0 \\ w_1 & 0 \\ 0 & 1 \\ 0 & w_2 \end{bmatrix}, \tag{13}$$
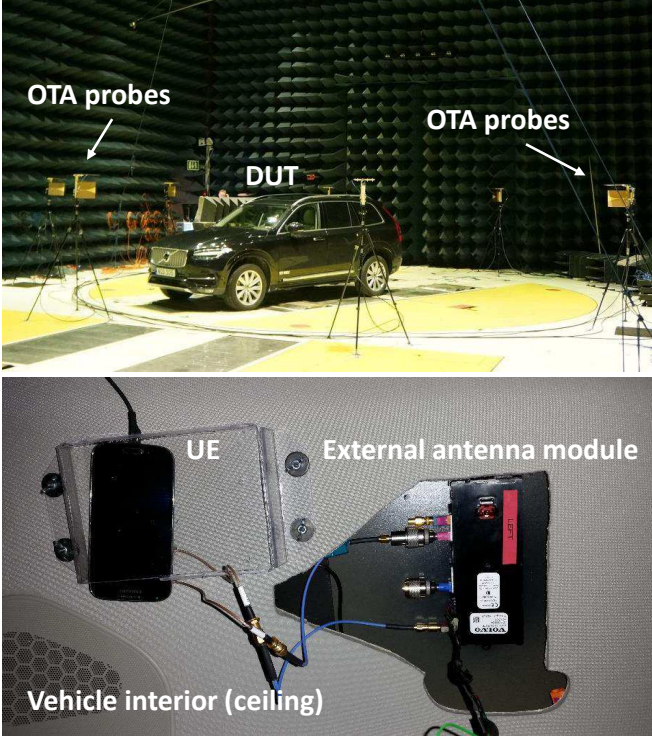
Fig. 3. A photo of the OTA measurement Setup. (Top) the measurement car with 8 dual-polarized OTA probes in the anechoic chamber; (bottom) the two-port external antenna module connected to an LTE device for throughput measurements.

Components	Specifications and settings
Base Station Emulator	• Model: Anritsu MT8820C. • Reference channel: R.35 FDD [23]. • Frame structure: frequency division duplex. • LTE frequency band: 1 (i.e. 2140 MHz). • Channel bandwidth: 10 MHz. • Transmission mode: 2×2 open loop MIMO.
Channel Emulator	• Model: Keysight PropSim F32. • BS antenna: 2 co-located $\pm 45°$ slanted isotropic dipoles [1]. • Channel model: SCME UMa and UMi channel model [16].
OTA Probes	• MPAC: 8 dual-polarized Vivaldi antennas evenly distributed on the OTA ring. • Wireless cable: 4 vertical-polarized antennas out of the 8 dual-polarized Vivaldi antennas. • OTA ring radius: 5 m.
DUT	• External antennas: Shark-fin antennas with 2 antenna elements under 3 setups as described in Section III-B. Element spacing: 80 mm. • UE: Samsung Galaxy S4. • Vehicle: Volvo XC 90. Dimensions: $495 \, cm \times 201 \, cm \times 178 \, cm$. • Metal sheet: Dimensions: $1 \, m \times 1 \, m$.

with two degrees of freedom w_1 and w_2. The upper two rows in (13) are responsible for establishing the wireless cable connection to the first Rx antenna on the DUT, and the lower two rows are for the connection to the second Rx antenna. The proper weights w_1 and w_2 are found sequentially for the first and the second wireless cable connection. To find the weight w_1, the lower two rows of $\boldsymbol{W}$ are set to zeros. The amplitude and phase of w_1 are tuned, and the received signal power RSRP on the two Rx antennas are reported. The isolation level for the first and the second wireless cable connection can be calculated as

$$\eta_1(w_1) = \frac{RSRP_1(w_1)}{RSRP_2(w_1)}, \tag{14}$$

$$\eta_2(w_2) = \frac{RSRP_2(w_2)}{RSRP_1(w_2)}, \tag{15}$$

respectively, where $RSRP_u$ denotes the RSRP value at the uth Rx branch with $u = \{1, 2\}$. The proper weight w_1 is found when the isolation level $\eta_1(w_1)$ achieves its maximum. Similarly, the proper weight w_2 for the second wireless cable connection can be found when $\eta_2(w_2)$ achieves its maximum with the upper two rows of $\boldsymbol{W}$ set to zeros. The isolation level is used as a metric to evaluate the quality of the wireless cable connections.

III. MEASUREMENT CAMPAIGN

A. Measurement Setup and Equipment

Photos of the measurement setup are given in Fig. 3. The measurements were performed in an anechoic chamber of di-

mensions $20.6 \, m \times 11.8 \, m \times 7.8 \, m$. In total, 8 dual-polarized OTA probes were evenly placed in the azimuth plane on a circle of 5 m in radius (OTA ring). Two-element shark-fin antennas were used as the DUT antennas, which were connected to a mobile phone (UE) to perform throughput measurements. The OTA probes were placed on the same hight of the DUT antennas at around 1.78 m above the floor. The measurements with the MPAC and the wireless cable method were both done with this setup. Table I details the equipment specifications and the measurement settings.

B. DUT antenna Setups

Three DUT setups are considered in the measurements, namely "Setup A", "Setup B", and "Setup C". In Setup A, a shark-fin antenna was mounted on a $1 \, m \times 1 \, m$ metal sheet. The shark-fin antenna consists of two antenna elements with around 80 mm spacing, which forms a two-port system. In Setup B, a shark-fin antenna of the same type was mounted on the roof of a car (of dimensions $495 \, cm \times 201 \, cm \times 178 \, cm$) at the regular position for vehicle antennas. In Setup C, two shark-fin antennas were mounted on the sides of the roof with around 81 cm spacing. In this setup, one element for each shark-fin antenna was used so that still a two-port system was formed but with a larger element spacing compared to Setup B. Photos of the three setups are given in Fig. 4. The center of the antenna was aligned to the center of the OTA ring in Setup A and B, while the geometry center of the two antennas was aligned to the center of the OTA ring in Setup C.

The antenna radiation pattern was measured for all three DUT setups in the same chamber, and the results are given in Fig. 5. Higher gain is observed in the V polarization for all setups, which indicates the measured shark-fin antennas are
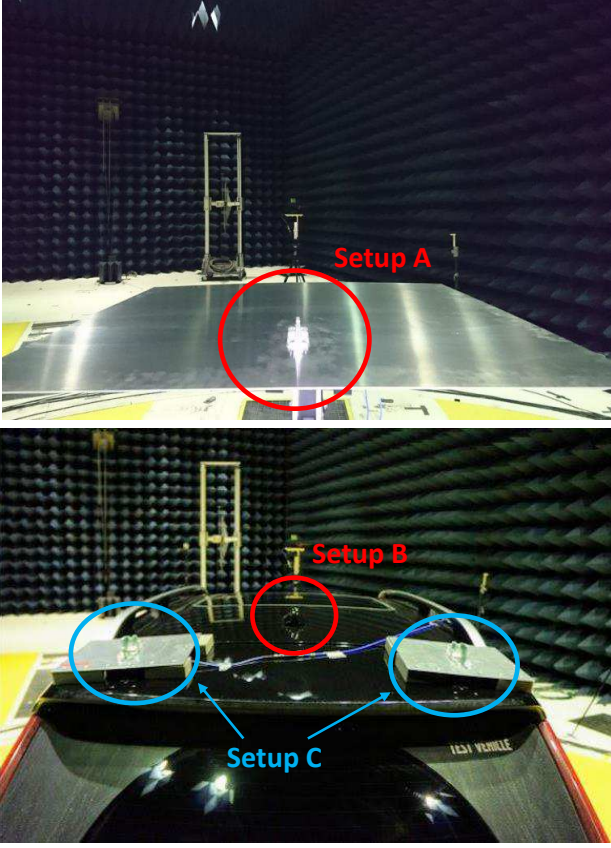
Fig. 4. Photos of the three DUT setups.

vertically polarized. Moreover, the measured antenna radiation pattern varies significantly among the three setups.

IV. MEASUREMENT RESULTS ANALYSIS

A. Synthetic Evaluation of the Emulation Accuracy for the MPAC Method

It is reported in the standard [1] that an 8-probe MPAC setup can support a test zone of 0.85λ (about $12\,\text{cm}$ at the testing frequency) in diameter for the target channel model, i.e. the SCME UMa and UMi model. This size is big enough to enclose one shark-fin antenna in our case. However, considering the ground plane in Setup A and the car in Setup B and Setup C, on which the induced surface current is distributed, the total size of the DUT including the ground plane or the car can be larger than the test zone. Therefore, it is necessary to verify the emulation accuracy under those conditions.

The three metrics discussed in Section II-B2, i.e. the average received power, the branch power ratio, and the antenna correlation at the DUT side were evaluated with the synthetic 8-probe (8P), 16-probe (16P), and 32-probe (32P) MPAC setup [24] according to (8) to (10). Recall that the size of the test zone is approximately proportional to the number of OTA probes [2]. Therefore, the 8P, 16P, and 32P MPAC setups correspond to the test zones of about $12\,\text{cm}$, $24\,\text{cm}$, and $48\,\text{cm}$ in diameter at the testing frequency, respectively, all of which are smaller than the maximum physical dimensions of the three DUT setups in the measurements.
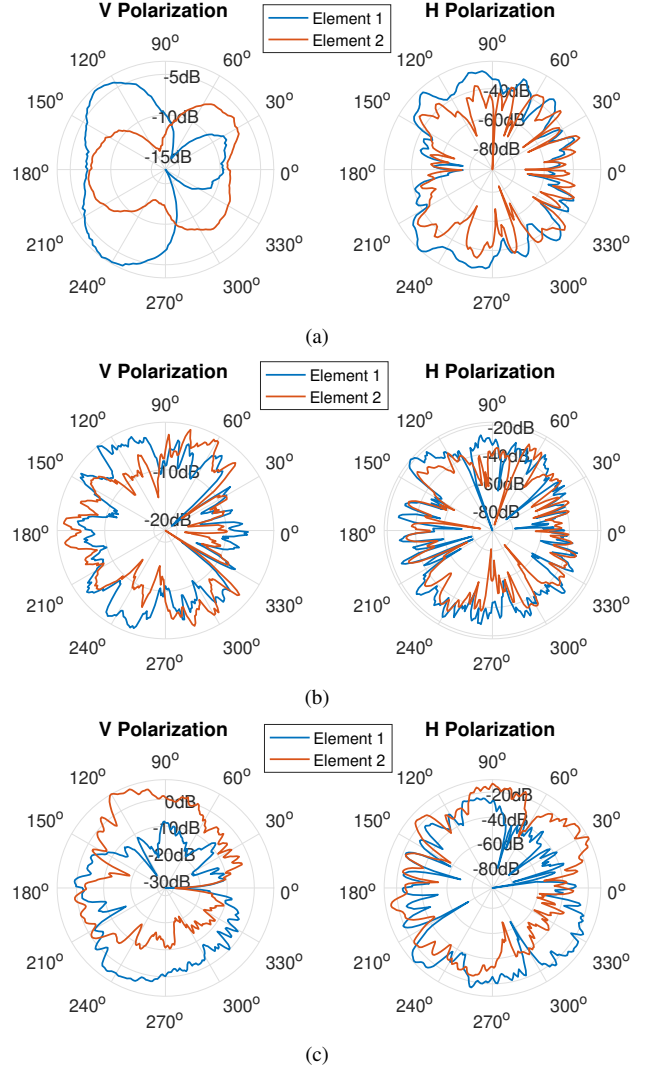

Fig. 5. Measured antenna radiation pattern for (a) Setup A, (b) Setup B, and (c) Setup C.

The values of the average received power and the branch power ratio under the target and the emulated channel for the three DUT setups are summarized in Table II. We can see that both the average received power and the branch power ratio under the emulated channel are quite close to the target values with a deviation up to around $1\,\text{dB}$, except for a deviation of around $2\,\text{dB}$ in the branch power ratio for Setup B under the UMa scenario with the 8P MPAC setup.

The target and the emulated antenna correlation, i.e. ρ and $\hat{\rho}$, are shown in the complex plane in Fig. 6 for the three DUT setups under the UMa and the UMi scenario. The deviation $|\rho - \hat{\rho}|$ against the number of OTA probes is further shown in Fig. 7. For Setup A (supposedly with the smallest effective antenna distance), the antenna correlation deviation is very small for different numbers of OTA probes with a deviation of about 0.03 for the 8P MPAC setup under the UMi scenario. For Setup B (supposedly with a median effective antenna distance), the emulated antenna correlation poses a deviation of about 0.2 with the 8P MPAC setup, but it approaches the target with the 16P MPAC setup. This indicates that the 8P

TABLE II
THE AVERAGE RECEIVED POWER AND THE BRANCH POWER RATIO OF THE TARGET AND THE EMULATED CHANNEL WITH THE SYNTHETIC 8-PROBE (8P), 16-PROBE (16P), AND 32-PROBE (32P) MPAC SETUP (UNIT: [dB]).

	SCME UMa														
	Setup A					Setup B					Setup C				
	8P	16P	32P	Target	Dev.	8P	16P	32P	Target	Dev.	8P	16P	32P	Target	Dev.
$\bar{P}_1$	−8.61	−8.59	N/A	−8.68	0.09	−7.84	−7.84	N/A	−6.70	1.14	−8.24	−8.46	−9.15	−8.62	0.53
$\bar{P}_2$	−9.10	−9.16	N/A	−8.99	0.17	−5.64	−6.08	N/A	−6.50	0.86	−2.82	−1.38	−1.68	−2.09	0.73
$\Delta\bar{P}$	0.49	0.57	N/A	0.31	0.26	2.20	1.76	N/A	0.20	2.00	5.42	7.08	7.46	6.53	1.11
	SCME UMi														
	Setup A					Setup B					Setup C				
	8P	16P	32P	Target	Dev.	8P	16P	32P	Target	Dev.	8P	16P	32P	Target	Dev.
$\bar{P}_1$	−9.36	−9.16	N/A	−9.34	0.18	−7.34	−8.42	N/A	−7.58	0.84	−6.38	−5.94	−6.83	−6.47	0.53
$\bar{P}_2$	−8.55	−8.34	N/A	−8.31	0.24	−7.42	−7.90	N/A	−7.90	0.48	−6.87	−5.43	−5.68	−5.97	0.90
$\Delta\bar{P}$	0.81	0.82	N/A	1.02	0.21	0.07	0.52	N/A	0.32	0.25	0.49	0.51	1.14	0.49	0.65

*The values for the emulated channels with the largest deviation to the corresponding target (denoted in blue) are denoted in red.

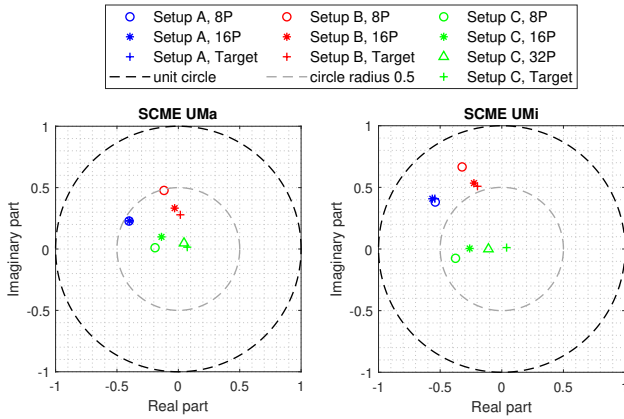**"Dev." denotes the absolute value of the largest deviation.

Fig. 6. DUT antenna correlation for the target and the emulated channel under (left) the SCME UMa scenario and (right) the SCME UMi scenario.
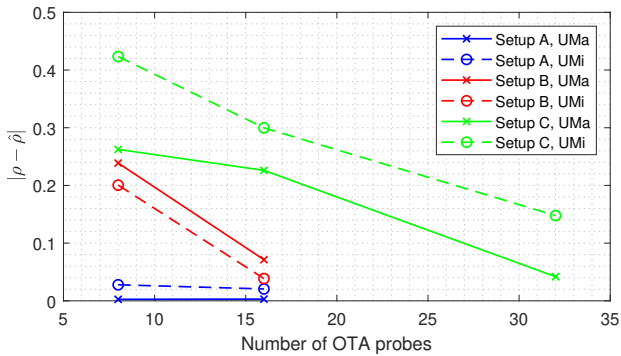

Fig. 7. Difference of the DUT antenna correlation between the target and the emulated channel under the UMa and UMi scenarios.

MPAC setup is not capable of accurately emulating the target spatial profile on the DUT side for Setup B. For Setup C (supposedly with the largest effective distance), the antenna correlation deviation decreases significantly with the increase of the number of OTA probes. This is expected since a larger number of OTA probes results in a larger size of the test zone.

However, similar to Setup B, the 8P MPAC is not capable of accurately emulating the target spatial profile on the DUT side for Setup C with an antenna correlation deviation of over 0.4 under the UMi scenario. Note that the three metrics under the 32P MPAC setup are not shown for Setup A and Setup B since the antenna correlation deviation $|\rho - \hat{\rho}|$ is already very small (below 0.1) for these two cases with the 8P and 16P MPAC setup, respectively (see Fig. 7).

B. Verification for the Wireless Cable Method

In our measurements, the amplitude of w_1 and w_2 was fixed to unity, and only their phase was tuned within the range $[-200°, 200°]$ to establish the wireless cable connections. The $RSRP_u$ with $u = \{1, 2\}$ was recorded against the phase of w_1 and w_2 as shown in Fig. 8. The red and the magenta circles denote the selected phase of w_1 and w_2 for the wireless cable connections with the maximum isolation level, respectively. A lowest isolation level of $\eta_2 = 6\,\mathrm{dB}$ was achieved for the wireless cable connection to the second Rx antenna in Setup B, whereas a highest isolation level of $\eta_1 = 22.1\,\mathrm{dB}$ was achieved for the connection to the first Rx antenna in Setup C. Note that in the standard [1], an isolation level of $18\,\mathrm{dB}$ is recommended for wireless cable connections; otherwise, interference from other wireless cable connections may influence the measurement results. Therefore, the throughput results for Setup A ($\eta_2 = 9.2\,\mathrm{dB}$) and Setup B ($\eta_2 = 6\,\mathrm{dB}$) might have suffered from a relatively high interference in the measurements. The low isolation that occurred in the measurements can be due to the phase-only tuning of W instead of both amplitude and phase tuning for establishing the wireless cable connections. Another possible cause is that the transfer function L was ill-conditioned, as the low isolation occurred for the two similar DUT setups, i.e. Setup A and Setup B, where the antenna element spacing is small.

C. Throughput Results Analysis

Throughput is a high-level metric which reflects the end-user experience directly. It is also used as a measure to check
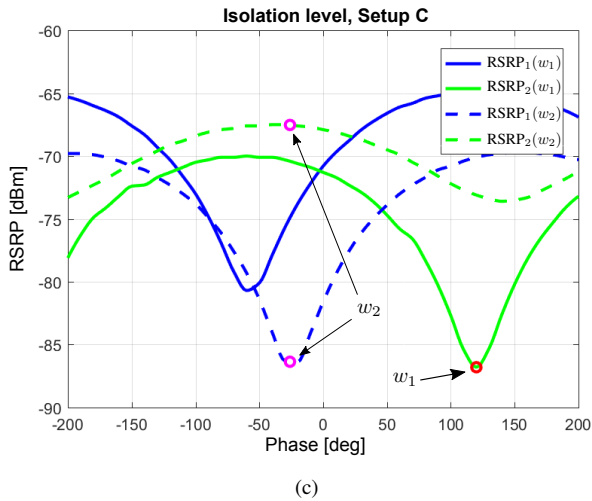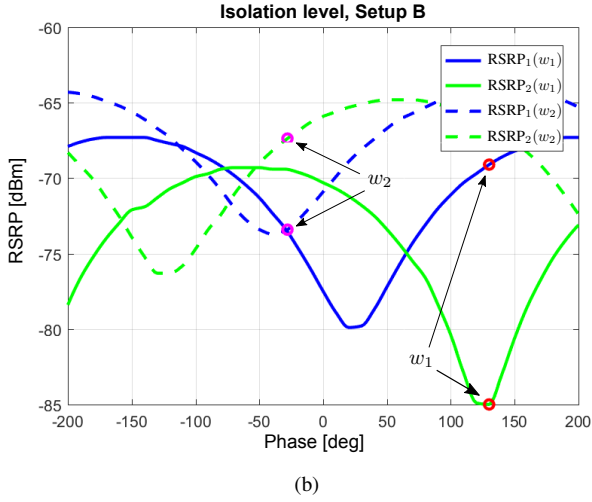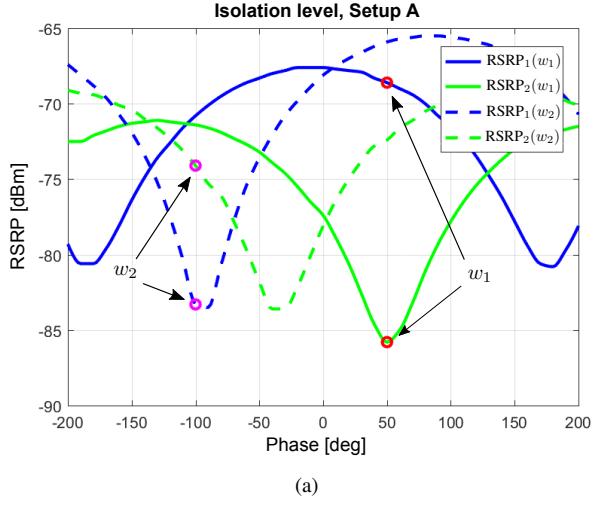
Fig. 8. Wireless cable connection established for (a) Setup A with an isolation level of $17.2\,\mathrm{dB}$ for the first Rx antenna and $9.2\,\mathrm{dB}$ for the second Rx antenna; (b) Setup B with an isolation level of $14.3\,\mathrm{dB}$ for the first Rx antenna and $6\,\mathrm{dB}$ for the second Rx antenna; (c) Setup C with an isolation level of $22.1\,\mathrm{dB}$ for the first Rx antenna and $19\,\mathrm{dB}$ for the second Rx antenna.
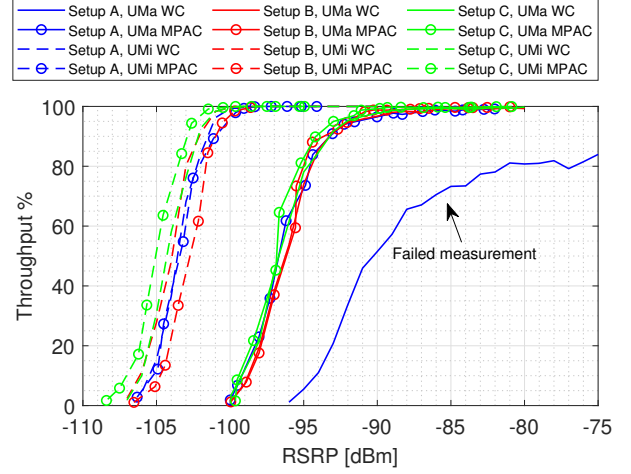

Fig. 9. Measured relative throughput against RSRP for the three DUT setups with the MPAC and the wireless cable (WC) method with 100% throughput corresponding to 35.424 Mbps.

the validity of different OTA methods [1]. In our case, the throughput performance is compared between the MPAC and the wireless cable method. The throughput measurements with the MPAC and the wireless cable method were done according to the standard MIMO OTA testing procedure described in [1]. The measurement results are shown in Fig. 9.

For the UMa scenario (the solid curves), the throughput results are in good agreement between the MPAC and the wireless cable method for Setup B and Setup C. The result of Setup A with the wireless cable method probably indicates a failed measurement due to some practical issues during the measurements, given the observation that the resulting throughput did not reach 100% even with a significantly high signal power (i.e. with $-75\,\mathrm{dBm}$ RSRP). As mentioned in Section IV-A, the 8P MPAC setup is not capable of accurately emulating the target channel for Setup B and Setup C. However, no significant difference in the measured throughput results between the MPAC and the wireless cable method is observed. This is probably due to the high antenna correlation at the BS side (i.e. 0.9 in magnitude) under the UMa scenario, which leads to an ill-conditioned target MIMO channel, and hence the throughput results are not sensitive to the antenna correlation at the DUT side [24]. Therefore, even when the antenna correlation deviation for the 8P MPAC setup is high (e.g. about 0.25 for Setup B, see Fig. 7), the emulation error is not reflected in the throughput results. Moreover, the measured throughput results are very similar among the three DUT setups for the same reason.

For the UMi scenario (the dashed curves), the throughput results are still in reasonably good agreement between the MPAC and the wireless cable method. Relatively large difference in the throughput results can be seen for Setup B and Setup C between the MPAC and the wireless cable method (e.g. with a difference up to $1.5\,\mathrm{dB}$ in RSRP for Setup B). In contrast to the UMa scenario, the magnitude of the antenna correlation at the BS side is 0.01 for the UMi scenario. Therefore, the throughput results are more dependent

on the antenna correlation at the DUT side. Consequently, the emulation error of the 8P MPAC setup is more noticeable under the UMi scenario in terms of the difference between the throughput results of the MPAC and the wireless cable method. However, it is interesting to point out that with an emulation deviation of around 0.4 in antenna correlation for Setup C under the UMi scenario (see Fig. 7), a relatively small difference of up to around $1\,\mathrm{dB}$ in RSRP is observed between the MPAC and the wireless cable method. It was found in [24] that antenna correlation deviation does not have a significant effect on throughput if the magnitudes of both the target and the emulated antenna correlation are below 0.5 under the UMi scenario, which explains the observation in our case.

Comparing the results between the UMa and the UMi scenarios, we can also see that the required RSRP for the same throughput percentage under the UMi scenario is always lower than that under the UMa scenario by about $5\,\mathrm{dB}$ for all three DUT setups, which indicates that a better throughput performance was achieved under the UMi scenario. This complies with our expectation due to the lower antenna correlation at the BS side for the UMi scenario [1], which is beneficial for spatial multiplexing for MIMO systems, and hence improves the throughput performance. Moreover, Setup C results in the best throughput performance under the UMi scenario as expected since the corresponding antenna correlation is the smallest among the three DUT setups (see Fig. 6).

In general, the difference in the throughput results between different DUT setups for each scenario is small. This is caused jointly by the underlying DUT antenna radiation pattern and the channel models. It can be inferred that the throughput is not very sensitive to the DUT setups and their respective emulation error in our measurement. Other types of DUT antennas and channel models can be considered to reflect more significantly their effect on the throughput.

D. Discussion on the MPAC and the Wireless Cable Setup for Car Testing

The MPAC setup is a true end-to-end MIMO OTA testing method. However, it suffers from a high system cost with the increase of the required test zone for large DUTs. As shown in Fig. 7, a 32P MPAC setup may be just adequate to emulate the target channel accurately, as for Setup C. The wireless cable setup may result in a lower cost compared to the MPAC setup, since the number of OTA probes for the wireless cable setup is not related to the size of the DUT but the number of the DUT antennas. However, due to the two-stage principle of the wireless cable setup, the DUT antenna radiation pattern is numerically implemented in the channel emulator. Therefore, the wireless cable setup is not for true end-to-end testing in principle. If DUT antenna patterns are non-adaptive as in the measurements, the wireless cable setup can approximate the true end-to-end testing. From the throughput results shown in Fig. 9, no significant difference in measured throughput between the MPAC and the wireless cable setup has been observed (except for the failed measurement). Therefore, the more cost-effective wireless cable setup is recommended for MIMO OTA testing for cars with non-adaptive DUT antenna patterns.

V. Conclusion

In this paper, the principles of two MIMO OTA testing methods, i.e. the MPAC and the wireless cable method, have been briefly revisited. One key question for performance testing for cars with the MPAC method is that to which extent the presence of vehicles will affect the required size of the test zone. Three DUT antenna setups are considered in the study, i.e. a two-element shark-fin antenna mounted on a $1\,\mathrm{m} \times 1\,\mathrm{m}$ ground plane (Setup A), a two-element shark-fin antenna on a car roof (Setup B), and two shark-fin antennas on the sides of the car roof with one element for each antenna being used (Setup C). The effect of the large ground plane and the car is accounted in the measured DUT antenna radiation pattern.

From the emulation accuracy point of view, different numbers of OTA probes do not lead to much deviation in the resulting average received power and branch power ratio with respect to the target values (with a deviation up to around $1\,\mathrm{dB}$). However, by the metric of the antenna correlation at the DUT side, the target channels can be well emulated with the 8P MPAC setup for the DUT Setup A, whereas more OTA probes (i.e. the 16P and the 32P MPAC setups) are needed for the DUT Setup B and Setup C, respectively. It can be inferred that the MPAC setup is capable of car testing but 16 or 32 OTA probes will be needed for a DUT antenna setup with large effective antenna distances to maintain a high emulation accuracy.

Moreover, throughput measurements have been performed with the 8P MPAC and the wireless cable setup under SCME UMa and UMi scenarios. A better throughput performance has been observed under the UMi scenario as expected. Except for the failed measurement, the throughput results from the MPAC and the wireless cable method are in good agreement (with a difference up to $1.5\,\mathrm{dB}$ in RSRP for Setup B under the UMi scenario). Furthermore, a better agreement is observed under the UMa scenario, due to the high antenna correlation of 0.9 in magnitude at the BS side under the UMa scenario, which results in an ill-conditioned MIMO channel. Hence the emulation error with the 8P MPAC setup in the antenna correlation at the DUT side does not affect the resulting throughput as much as it does under the UMi scenario. Given the similarity of the throughput results between the MPAC and the wireless cable setup, the more cost-effective wireless cable setup is recommended for car testing with non-adaptive DUT antenna patterns.

References
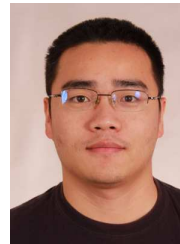
[1] 3GPP, "Verification of radiated multi-antenna reception performance of User Equipment (UE)," Technical Specification Group Radio Access Network, Tech. Rep. 3GPP TR 37.977 V14.3.0, 2017.

[2] P. Kyösti, T. Jämsä, and J.-P. Nuutinen, "Channel modelling for multiprobe over-the-air MIMO testing," *International Journal of Antennas and Propagation*, vol. 2012, 2012.

[3] W. Fan, P. Kyösti, L. Hentilä, and G. F. Pedersen, "MIMO Terminal Performance Evaluation With a Novel Wireless Cable Method," *IEEE Transactions on Antennas and Propagation*, vol. 65, no. 9, pp. 4803–4814, 2017.

[4] X. Chen, J. Tang, T. Li, S. Zhu, Y. Ren, Z. Zhang, and A. Zhang, "Reverberation Chambers for Over-the-Air Tests: An Overview of Two Decades of Research," *IEEE Access*, vol. 6, pp. 49 129–49 143, 2018.

[5] D. Micheli, M. Barazzetta, R. Diamanti, P. Obino, R. Lattanzi, L. Bastianelli, V. M. Primiani, and F. Moglie, "Over-The-air tests of high-speed moving LTE users in a reverberation chamber," *IEEE Transactions on Vehicular Technology*, vol. 67, no. 5, pp. 4340–4349, 2018.

[6] 3GPP, "Study on LTE Support for V2X Services," Tech. Rep. 3GPP TR 22.885 V1.0.0, 2015.

[7] M. G. Nilsson, P. Hallbjörner, N. Arabäck, B. Bergqvist, T. Abbas, and F. Tufvesson, "Measurement Uncertainty, Channel Simulation, and Disturbance Characterization of an Over-the-Air Multiprobe Setup for Cars at 5.9 GHz," *IEEE Transactions on Industrial Electronics*, vol. 62, no. 12, pp. 7859–7869, 2015.

[8] P. Berlt, C. Bornkessel, and M. A. Hein, "Spatial Correlation of C-V2X Antennas Measured in the Virtual Road Simulation and Test Area," in *12th European Conference on Antennas and Propagation (EuCAP 2018)*, 2018, pp. 1–5.

[9] C. Schirmer, M. Lorenz, W. A. Kotterman, R. Perthold, M. H. Landmann, and G. Del Galdo, "MIMO over-the-air testing for electrically large objects in non-anechoic environments," in *2016 10th European Conference on Antennas and Propagation, EuCAP 2016*. European Association of Antennas and Propagation, 2016, pp. 1–6.

[10] M. Schilliger Kildal, J. Kvarnstrand, J. Carlsson, A. A. Glazunov, A. Majidzadeh, and P.-S. Kildal, "Initial Measured OTA Throughput of 4G LTE Communication to Cars with Roof-Mounted Antennas in 2D Random-LOS," in *2015 International Symposium on Antennas and Propagation (ISAP)*, 2015, pp. 1–4.

[11] M. S. Kildal, J. Carlsson, and A. Alayon Glazunov, "Measurements and simulations for validation of the random-LOS measurement accuracy for vehicular OTA applications," *IEEE Transactions on Antennas and Propagation*, vol. 66, no. 11, pp. 6291–6299, 2018.

[12] A. Razavi, A. A. Glazunov, P. S. Kildal, and R. Maaskant, "Array-fed cylindrical reflector antenna for automotive OTA tests in Random Line-Of-Sight," in *2016 10th European Conference on Antennas and Propagation, EuCAP 2016*, 2016, pp. 3–6.

[13] R. K. Sharma, C. Schneider, W. Kotterman, G. Sommerkorn, P. Grosse, F. Wollenschlager, G. Del Galdo, M. A. Hein, and R. S. Thoma, "Over-the-air testing of Car-to-Car and car-to-infrastructure communication in a virtual electromagnetic environment," in *IECON Proceedings (Industrial Electronics Conference)*, 2013, pp. 6897–6902.

[14] M. G. Nilsson, C. Gustafson, T. Abbas, and F. Tufvesson, "A Measurement-Based Multilink Shadowing Model for V2V Network Simulations of Highway Scenarios," *IEEE Transactions on Vehicular Technology*, vol. 66, no. 10, pp. 8632–8643, 2017.

[15] ——, "A path loss and shadowing model for multilink vehicle-to-vehicle channels in urban intersections," *Sensors*, vol. 18, no. 12, pp. 1–19, 2018.

[16] D. S. Baum, J. Hansen, G. D. Galdo, and M. Milojevic, "An Interim Channel Model for Beyond-3G Systems," *Vehicular Technology Conference, 2005. VTC 2005-Spring. 2005 IEEE 61st*, vol. 5, pp. 3132–3136, 2005.

[17] 3GPP, "Spatial channel model for Multiple Input Multiple Output (MIMO) simulations," Tech. Rep. 3GPP TR 25.996 V12.0.0, 2014.

[18] WINNER, "WINNER II Channel Models: Part I Channel Models," Tech. Rep. D1.1.2 V1.2, 2007.

[19] 3GPP, "Study on channel model for frequencies from 0.5 to 100 GHz," Tech. Rep. 3GPP TR 38.901 V14.0.0, 2017.

[20] P. Bello, "Characterization of Randomly Time-Variant Linear Channels," *IEEE Transactions on Communications Systems*, vol. 11, no. 4, pp. 360–393, 1963.

[21] Y. Ji, W. Fan, G. F. Pedersen, and X. Wu, "On Channel Emulation Methods in Multiprobe Anechoic Chamber Setups for Over-the-Air Testing," *IEEE Transactions on Vehicular Technology*, vol. 67, no. 8, pp. 6740–6751, 2018.

[22] W. Fan, P. Kyösti, Y. Ji, L. Hentilä, X. Chen, and G. F. Pedersen, "Experimental Evaluation of User Influence on Test Zone Size in Multiprobe Anechoic Chamber Setups," *IEEE Access*, vol. 5, 2017.

[23] 3GPP, "Evolved Universal Terrestrial Radio Access (E-UTRA); User Equipment (UE) radio transmission and reception," Tech. Rep. 3GPP TS 36.101 V15.7.0, 2019.

[24] W. Fan, L. Hentilä, P. Kyösti, and G. F. Pedersen, "Test Zone Size Characterization with Measured MIMO Throughput for Simulated MPAC

Configurations in Conductive Setups," *IEEE Transactions on Vehicular Technology*, vol. 66, no. 11, pp. 10 532–10 536, 2017.
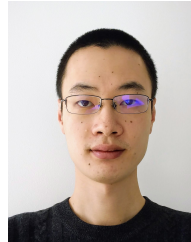
Yilin Ji was born in 1991 in Shanghai, China. He received his B.Sc. degree in Electronics Science and Technology and M.Eng degree in Integrated Circuit Engineering from Tongji University, China, in 2013 and 2016, respectively. He is currently a Ph.D. fellow at the Antennas, Propagation and Millimeter-wave Systems (APMS) section at Aalborg University, Denmark. His main research areas are radio propagation channel and MIMO OTA testing.

Wei Fan received his Bachelor of Engineering degree from Harbin Institute of technology, China in 2009, Master's double degree with highest honours from Politecnico di Torino, Italy and Grenoble Institute of Technology, France in 2011, and Ph.D. degree from Aalborg University, Denmark in 2014. From February 2011 to August 2011, he was with Intel Mobile Communications, Denmark as a research intern. He conducted a three-month internship at Anite telecoms oy, Finland in 2014. His main areas of research are over the air testing of multiple antenna systems, radio channel sounding, modelling and emulation. He is currently an associate professor at the Antennas, Propagation and Millimeterwave Systems (APMS) Section at Aalborg University.

Mikael G. Nilsson (M'09) received the Ph.D. degree from Lund University, Lund, Sweden, in 2018. From 1997 to 2003, he worked mostly as a consultant within the telecommunications and space industry. In 2003, he joined Volvo Car Corporation, Göteborg, Sweden, where he held various positions and, since 2012, has been a Technical Expert for Wireless Communication. He is dedicated to the Six Sigma methodology and has been teaching several Design for Six Sigma and Green Belt courses within Volvo Car Corporation. His principal research areas are channel characterization of the 5.9-GHz band and measurement systems, namely, the over-the-air multiprobe setup for cars.

Lassi Hentilä was born in 1978 in Oulu Finland. He received his M.Sc. in electrical engineering, telecommunications, from the University of Oulu Finland, in 2004. He worked from 2001 to 2004 in Centre for Wireless Communications (CWC) at Oulu University. In 2004, he moved to Elektrobit where he worked on radio propagation, radio channel measurements and modeling, MIMO OTA research and standardization and participated in the European IST-WINNER projects (WINNER I, WINNER II and WINNER+). In 2013, he moved to Anite Telecoms Oy where he worked as a MIMO OTA specialist. In 2016, he moved to Keysight Technologies Oy as a part of the acquisition of Anite. In Keysight he develops OTA and solutions for 5G base station and mobile station testing.

Kristian Karlsson was born in Borås, Sweden, in 1973. He received the M.Sc.E.E. degree in applied physics and electrical engineering from Linköpings University of Technology, Linköping, Sweden, in 1998. From 1998 to 2001 he was a software development engineer at first ÅF industriteknik AB and then TietoEnator AB, both Sweden. From 2001 he is employed by RISE Research Institutes of Sweden. Initially as a responsible for Swedish national measurement site of radiated electromagnetic fields and later as a researcher. He received his Ph.D. in 2009 from Chalmers University of Technology, Gothenburg, Sweden. His primary research interests are in electromagnetics, antenna systems, vehicle to vehicle communications and automotive radar systems. He has authored or coauthored more than 30 papers in IEEE journals and conferences, concerning antenna systems, wireless communications and automotive radar. Dr. Karlsson is a member of the Swedish National Committee for Radio Science, Section A. He has been a reviewer for the IEEE Transactions on antennas and propagation and several IEEE conferences.

Fredrik Tufvesson received his Ph.D. in 2000 from Lund University in Sweden. After two years at a startup company, he joined the department of Electrical and Information Technology at Lund University, where he is now professor of radio systems. His main research interest is the interplay between the radio channel and the rest of the communication system with various applications in 5G systems such as massive MIMO, mm wave communication, vehicular communication and radio based positioning. Fredrik has authored around 90 journal papers and 140 conference papers, he is fellow of the IEEE and recently he got the Neal Shepherd Memorial Award for the best propagation paper in IEEE Transactions on Vehicular Technology and the IEEE Communications Society best tutorial paper award.

Gert Frølund Pedersen was born in 1965. He received the B.Sc. and E.E. (Hons.) degrees in electrical engineering from the College of Technology, Dublin Institute of Technology, Ireland, in 1991, and the M.Sc.E.E. and Ph.D. degrees from Aalborg University, Aalborg, Denmark, in 1993 and 2003, respectively. Since 1993, he has been with Aalborg University where he is a Full Professor heading the Antennas, Propagation and Millimeter-wave Systems LAB with more than 35 researchers. He has also been the Head of the Doctoral School on wireless communication with some 40 Ph.D. students enrolled, from 2009 to 2019. His research interests include radio communication for mobile terminals especially small antennas, diversity systems, propagation, and biological effects. He has published more than 500 peer-reviewed papers, several books and book chapters and holds more than 50 patents. He has also worked as a consultant with developments of more than 100 antennas for various equipment etc.. This include the first internal antenna for mobile phones in 1994 with lowest SAR, the first internal triple-band antenna in 1998 with low SAR and high TRP and TIS, and lately various multiantenna systems rated as the most efficient on the market. He has worked most of the time with joint university and industry projects and have received more than 25 M$ in direct research funding. He is currently the Project Leader of the RANGE project with a total budget of over 8 M$ investigating high performance centimeter/ millimeter-wave antennas for 5G mobile phones. He has been the pioneer in establishing over-the-air measurement systems. The measurement technique is now well established for mobile terminals. He was chairing the various COST groups with liaison to 3GPP and CTIA for over-the-air test methods. He is currently heavily involved in SMART compact millimeter-wave antennas for 5G, for nano-satellites and for small satellite terminals as well as research into antenna and OTA measurement. He has lately established a very large antenna measuring facility at the university capable of measuring on systems from 100 MHz to THz and objects up to 3500 KG.